

UNCLASSIFIED

AD

204816

FOR  
MICRO-CARD  
CONTROL ONLY

1 OF 1

Reproduced by

Armed Services Technical Information Agency

ARLINGTON HALL STATION; ARLINGTON 12 VIRGINIA

UNCLASSIFIED

"NOTICE: When Government or other drawings, specifications or other data are used for any purpose other than in connection with a definitely related Government procurement operation, the U.S. Government thereby incurs no responsibility, nor any obligation whatsoever; and the fact that the Government may have formulated, furnished, or in any way supplied the said drawings, specifications or other data is not to be regarded by implication or otherwise as in any manner licensing the holder or any other person or corporation, or conveying any rights or permission to manufacture, use or sell any patented invention that may in any way be related thereto."

AD No. 204816

ASTA FILE COPY

**FC**

A Study of Vibrational Relaxation in  
Carbon Monoxide by Shock-waves and Infra-red Emission

by Mr. Winicor, Mr. Davidson and R. Taylor

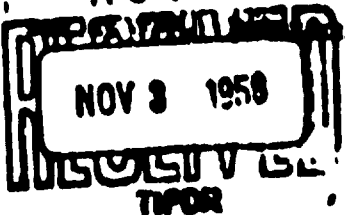
California Institute of Technology  
Pasadena, California

## Introduction

The interchange of energy between external degrees of freedom (translation) and the internal degrees of freedom (vibration and rotation) of a molecule when it undergoes a collision, is a subject of great importance, because of its intrinsic interest, because of its significance in the general field of chemical kinetics, and because of its bearing on various gas dynamical and combustion problems. When a gas is suddenly heated, as for example, by a shock-wave, or suddenly cooled, as by a rapid expansion, it undergoes a rapid change in temperature. In our normal usage of the term "temperature" we mean that the kinetic energy of translation of the molecules has changed. If the change is very sudden, the new distribution of molecular velocities may instantaneously even no longer follow the Maxwell-Boltzmann law. A new Boltzmann distribution is established in the time of a few collisions. To achieve complete thermodynamic equilibrium, it is now necessary for the energies of the rotational and the vibrational degrees of freedom to become adjusted. This will involve a further change of temperature as interchange of energy between translation and rotation and vibration takes place. The collisional processes by which this equilibration is effected are called rotational or vibrational relaxation.

Rotational relaxation usually takes only a few to a few tens of microseconds, corresponding to a time of about  $10^{-10}$  seconds.

## Best Available Copy



translation may, for most purposes therefore, be grouped together as external degrees of freedom. The transfer of energy between vibrations and external degrees of freedom, on the other hand, often turns out to be a very inefficient process. This is especially so for simple stiff diatomic molecules such as nitrogen, where many hundreds of thousands or even millions of collisions may be required. The relaxation time is long enough to make the question of vibrational relaxation assume practical importance. It affects, for example, the state of a gas undergoing rapid expansion in a rocket nozzle or suffering rapid compression behind a shock-wave.

With increasing molecular complexity, vibrational relaxation is more rapid, less than 20 collisions being required for propane at 20°C and 1 atm. It is still not uncommon, however, to find several thousand collisions necessary and in special cases, as in CO<sub>2</sub> at room temperature, the relaxation time may still be as long as several microseconds.

These statements apply to the pure gas. The study of molecules with long relaxation times is almost always complicated by the fact that polyatomic molecules usually make much more efficient collision partners for relaxation than another molecule of the pure gas. Minute amounts of polyatomic impurities may therefore reduce the observed times by several orders of magnitude. The commonest contaminant is water vapor and the problem of its removal will be discussed later on.

A number of methods have been employed for measuring relaxation times. These include: (1) the dispersion and absorption of ultrasonic waves,<sup>1</sup> (2) the impact tube,<sup>1</sup> (3) interferometric measurements of density changes behind shock-waves,<sup>1,2</sup> (4) a direct method involving infra-red radiation, called the spectrophone technique,<sup>3</sup> (5) the infra-red emission method described here.

In the present work a new technique for measuring vibrational relaxation times has been developed.<sup>4</sup> The rate of population of a particular vibrationally excited state in a gas that has been rapidly heated by the passage of a shock-wave is followed by observing the emission of infra-red radiation from this state with a detector of short response time.

In the particular application described here, we observe the rate of population of the 2 d vibrational state ( $v = 2$ ) of CO from the time dependence of the emission of the first overtone ( $2 \rightarrow 0$ ) radiation at  $2.335 \mu$ . (To some extent, of course, one is also looking at the transitions,  $3 \rightarrow 1$ ,  $4 \rightarrow 2$ , etc., and hence at the population of these upper states.) The radiative lifetime for the  $2 \rightarrow 0$  transition is 1.1 sec.<sup>5</sup> At equilibrium at 1 atm at  $1500^{\circ}\text{K}$  the calculated emission is  $7.2 \times 10^{-3}$  watts  $\text{cc}^{-1}$ , which, in the experimental arrangement, is readily detected. It is difficult to calculate self-absorption accurately, but approximate calculations according to the method of Penner and Weber<sup>6</sup> indicate that it is small or negligible (Actually, the amount of radiation is proportional to the population of the  $v = 2$  state even if there is self-absorption provided that the amount of self-absorption is fairly constant; and specifically if it is not large in the boundary layer where the density and temperature are quite different than that of the bulk gas.) The lifetime for the  $2 \rightarrow 1$  transition is 0.015 sec<sup>5</sup>; in our experiments, the lifetime for the  $2 \rightarrow 0$  overall transition by collision is  $10^{-3}$  sec or less. Therefore, the radiative processes serve to indicate the population of the state without significantly affecting it.

### Experimental

The Shock Tube. The use of the shock tube in this laboratory as a tool for studying chemical reactions at high temperatures has already been described.<sup>7</sup> In all of our previous work the progress of a chemical reaction has been followed by the absorption of visible or ultraviolet light.

The length of our shock tube has been increased in order to improve the quality of the shocks and to increase the time available for observations. The diameter is 15 cm; the driving section is a 270 cm length of aluminum pipe; the shock wave section consists of a 140 cm length of aluminum pipe and two 150 cm lengths of pyrex pipe.

Part of the motivation to lengthen the tube was the desire to make observations in the region behind the reflected shock front which would have previously been terminated far too soon by the arrival of disturbances from the driving section. Reflected shock studies have several advantages. In the first place, the gas behind the reflected shock is stationary, so that the time-compression effect associated with the fact that the gas behind the incident shock is moving, does not occur. The removal of this penalty was important since our detector was already a limiting factor and we could ill afford to sacrifice any of its limited response time. Secondly, almost a millisecond was available before the arrival of the cold front. Finally, due to the double compression and heating, high temperatures and pressures could be reached without excessively high driving pressures and using less carbon monoxide. All of the experimental results presented here were made using the reflected shock technique. The observation station was set up as close as possible to the end-plate to minimize disturbances due to the growth of the boundary layer and to get the maximum observation time. The distance

chosen was 3 cm. With the optical system employed, this was enough to prevent the detector seeing possible radiation from the end-plate.

The Infra-red Cell. A lead sulfide photoconductive detector made by The Electronics Corporation of America was used. The sensitive element was 3 mm by 3 mm. The response time was  $1.7 \pm 3 \mu\text{sec}$ ; the cell resistance was 6 megohms; the sensitivity was  $1.5 \times 10^4$  volts/watt; and the noise equivalent power (at 5 cps) was ca.  $3 \times 10^{-11}$  watts. The associated electronics did not increase the rise time. The output of the detector was fed into a preamplifier and then to an oscilloscope. The cell was mounted in a turret setting with three-way movement for focussing. A germanium filter cut off radiation below  $2.0 \mu$  and the pyrex wall of the shock tube absorbed radiation larger than  $2.8 \mu$ . In addition, a Corning filter No. 3434 with a long wave length cut off at  $2.6 \mu$  was used. This effectively isolated radiation from the  $0 \rightarrow 2$  transition in carbon monoxide which is centered at  $2.335 \mu$ . In control experiments with dry nitrogen, less than 4 percent emission was observed. The experimental layout is shown in Fig. 1.

Fig. 1 here

This also shows schematically the schlieren systems which were used for starting and stopping the timer and triggering the oscilloscopes.

The removal of impurities. Early work served to emphasize the importance of excluding water vapor and other impurities from the system due to the very high efficiency of these molecules as collision partners for the relaxation process. Two measures were necessary: (a) the use of carbon monoxide of very high purity, (b) the reduction of the static pressure of  $\text{H}_2\text{O}$  or  $\text{CO}_2$  in the shock tube, caused by desorption from the walls, to as low a level as possible.

One series of experiments was made with Matheson Assayed Reagent Grade CO. Mass spectrometric analyses were supplied and listed the main impurities in two samples as carbon dioxide, 0.04 and 0.27 mole percent, and hydrogen, 0.03 and 0.02 mole percent. Most of the work was done with samples prepared by fractional distillation of Matheson C.P. grade carbon monoxide in a good low temperature column with a reflux head refrigerated with pumped down liquid nitrogen. This gave quite pure CO. A typical mass spectrometer analysis (Consolidated Electrodynamics Co.) is: O<sub>2</sub>, 10<sup>-4</sup> mole percent, H<sub>2</sub>O, less than .015 mole percent, all other impurities less than .005 mole percent.

The other source of impurities was the walls of the shock tube. To combat this three measures were adopted. (a) The whole low-pressure section of the shock-tube, except for the observation area, was wound with a heating element. A temperature of 50 to 70°C could then be maintained while pumping out the tube to facilitate outgassing. (b) A false end-plate was designed fitted with a re-entrant cold finger which could be refrigerated with liquid nitrogen or other coolant. During evacuation a hole in the false end-plate gave access from the main volume of the tube to the cold finger which lay between the true end and the false end. Before starting a run, this hole was filled by pushing in a plug, the shaft of which extended through the tube end-plate via a hole sealed with an O-ring. The end-plate also carried a mounting for a Phillips ionization gauge. (c) The pumping arrangements for the tube, which now has a volume of about 80 liters, were improved by installing a three-stage oil diffusion pump connected to the tube via a high-speed, one-inch aperture baffle valve.

With the aid of these improvements, it was possible to achieve a pressure of about  $10^{-5}$  mm Hg with liquid nitrogen in the cold finger. The pressure rise with the shock-tube isolated was less than  $10^{-6}$  mm per minute. Since a run takes about 10 minutes, this is negligible with the amounts of gas used. For experiments with added  $\text{CO}_2$ , the cold finger was filled with dry ice and trichlorethylene, and a control experiment was made under these conditions without added  $\text{CO}_2$ . Mixtures of CO and  $\text{CO}_2$  were made up beforehand in a storage bulb. For experiments with added  $\text{H}_2\text{O}$ , either dry ice as above or methylene bromide at its freezing point was employed. The technique adopted was to admit excess water vapor to the tube first and then let in the CO. About 15 minutes was allowed for the  $\text{H}_2\text{O}$  to come to equilibrium with the ice on the cold finger and to mix with the CO. The vapor pressure of  $\text{H}_2\text{O}$  is 0.06  $\mu$  at  $-78^\circ\text{C}$  (dry ice) and about 50  $\mu$  at  $-50^\circ\text{C}$  (melting methylene bromide). Control runs without added  $\text{H}_2\text{O}$  were done at each temperature.

Calculation of Temperature and Pressure. The temperature and density of a shocked gas can be calculated from the shock velocity and the initial conditions if the enthalpy of the gas is known as a function of temperature. As vibrational relaxation occurs behind a strong shock, the temperature decreases and the density increases. The situation is more complicated for reflected shocks. We have calculated the conditions behind the reflected shock from the measured velocity of the incident shock. We assume, in accordance with the evidence, that the gas behind the incident shock is unrelaxed. Calculations have been made for the unrelaxed incident -

unrelaxed reflected condition. This is strictly applicable to the reflected shock very close to the end plate. Calculations could also be made for the unrelaxed incident-relaxed reflected conditions. This would be appropriate for the steady state shock after a long period of time. One is however observing the process of vibrational relaxation close to the end plate. Neither of the above limiting steady flow conditions therefore applies. The gas behind the shock is contracting and the resulting rarefaction wave is moving out to merge with and slow down the shock. A correct calculation would be very complicated. We have therefore used the unrelaxed-unrelaxed calculations of temperature and density. Fortunately, the vibrational enthalpy is not too large and the uncertainties are small.

Examples of reflected shock calculations are given in Table I.

Table 1. Typical Shock Parameters in CO

$T_1$ °K	$s_1$ cm/msec	$\Pi_1$	$\Delta_1$	$T_r$ °K	$s_r$ cm/msec	$\Pi_r$	$\Delta_r$	$\Pi_t$	$\Delta_t$
500	60.97	4.44	2.65	73	35.13	3.31	2.04	14.7	5.03
600	83.47	6.34	3.18	96	37.72	4.05	2.50	15.9	7.00
700	105.23	8.37	3.57	119	40.42	4.50	2.70	17.4	9.61
800	105.3	10.36	3.86	140	43.06	5.01	2.82	18.9	10.80
900	115.4	12.36	4.09	164	45.61	5.33	2.91	19.9	11.32
1000	124.0	14.36	4.28	186	48.22	5.60	2.97	20.4	12.70
1100	132.3	16.34	4.43	212	50.84	5.83	3.02	21.4	13.36
1200	140.2	18.35	4.56	234	53.77	6.00	3.07	22.0	14.00
1300	147.6	20.36	4.67	256	54.91	6.14	3.11	22.6	14.50
1400	154.8	22.40	4.77	280	56.20	6.28	3.14	23.5	14.93
1500	161.6	24.40	4.85	301	58.33	6.40	3.17	24.0	15.31

$T_r$ , temperature of heated gas behind shock;  $s$ , shock velocity;  $\Pi$ , pressure ratio across shock;  $\Delta$ , density ratio across shock. Subscript  $1$  refers to incident shock, subscript  $r$  refers to reflected shock, and subscript  $t$  refers to total change.

Results

The vibrational relaxation time of carbon monoxide has been measured between  $1400^{\circ}\text{K}$  and  $3000^{\circ}\text{K}$  and over a range of final pressures from 1 to 3.5 atm. A preliminary study of the effect of small amounts of  $\text{CO}_2$  and  $\text{H}_2\text{O}$  has also been made.

A typical experimental record of infra-red emission due to the  $2 \rightarrow 0$  transition is shown in Fig. 2.

Fig. 2 here

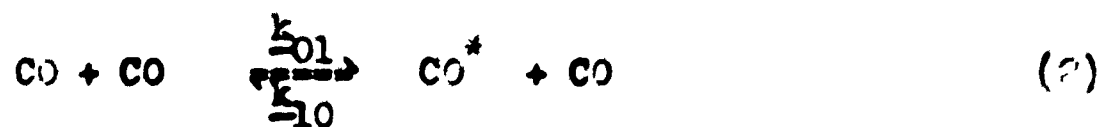
As indicated previously, it is believed that the intensity of the emission is directly proportional to the concentration of molecules in the upper state. After a small initial region of gradually increasing slope, the trace rises almost linearly for about half the total amplitude and then approaches the equilibrium value asymptotically.

Interpretation. One may conceive of any one of three possibilities as being the most important path for populating the state  $v = 2$ .

There is the direct  $0 \rightarrow 2$  excitation



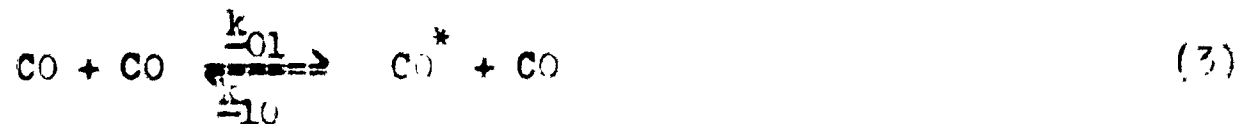
There is a two step process,  $0 \rightarrow 1 \rightarrow 2$ .



There is also the possibility (3), in which two  $\text{CO}^*$  molecules react to give  $\text{CO}^{**} + \text{CO}$ , in which no conversion of translational energy to vibra-

tional energy occurs, but in which the vibrational energy is redistributed.

For this process the forward and reverse rate constants,  $\underline{k}$ , are equal.



For simplicity, make the approximation  $(\text{CO}^{**}) \ll (\text{CO}^*) \ll (\text{CO})$ .

Hypothesis (1) gives a simple exponential growth of  $(\text{CO}^{**})$ .

$$(\text{CO}^{**}) = (\text{CO}^{**})_{\infty} \left\{ 1 - \exp \left[ -\underline{k}_{20}(\text{CO})t \right] \right\} \quad (1a)$$

In the harmonic oscillator approximation,  $\underline{k}_{12} = 2\underline{k}_{01}$ ,  $\underline{k}_{21} = 2\underline{k}_{10}$ .

Then hypothesis (2) gives

$$(\text{CO}^{**}) = (\text{CO}^{**})_{\infty} \left\{ 1 - \exp \left[ -\underline{k}_{10}(\text{CO})t \right] \right\}^2 \quad (2a)$$

If in hypothesis (3), we assume  $\underline{e}$  is very large, expression (2a) again results. Thus, (1) gives a simple exponential growth, beginning with a finite slope, whereas (2) and (3) give growth beginning with zero slope, then rising steeply, with a rise time of the order of  $1/\underline{k}_{10}(\text{CO})$ , namely the relaxation time of the first vibrational state.

Hypothesis (3) can be discussed in further detail as follows. Reactions like (3a) are "energy transfers at exact resonance." The complete set of such reactions do not create vibrational energy, but they redistribute it in such a way that the population of the  $n$ 'th level,  $(\text{CO}^{n*})$ , is related to the population of the first excited level by

$$(\text{CO}^{n*}) = (\text{CO}^*)^n \left( \frac{E_{\text{vib}}}{h\nu + E_{\text{vib}}} \right) \left( \frac{h\nu}{h\nu + E_{\text{vib}}} \right)$$

That is, there is a Boltzmann-like distribution determined by the total amount of vibrational energy,  $E_{vib}$ , in the system. Given such a Boltzmann-like distribution, reactions like (3a) will be proceeding backward and forward at equal rates and will not further affect the distribution. Now, Montroll and Shuler<sup>9</sup> have shown that if one considers the complete set of equations like (2) in the harmonic oscillator approximation, then a system which starts with a Boltzmann distribution of vibrational states appropriate to one temperature relaxes to the Boltzmann distribution appropriate to the translational temperature via a set of Boltzmann distributions appropriate to intermediate temperatures. Under these circumstances, the reaction system (3a) makes no contribution to the vibrational distribution even though its rate constant may be large.

Plots of  $\ln\left\{1 - (CO^{**})/(CO)_{\infty}^{**}\right\}$  vs.  $\underline{t}$  and of  $\ln\left\{1 - \left[(CO^{**})/(CO)_{\infty}^{**}\right]^{1/2}\right\}$  vs.  $\underline{t}$  are shown in Fig. 3. The latter relation gives a better straight line, thus favoring hypothesis (2) or (3). The situation is not perfectly

Fig. 3 here

clear cut however because the finite rise time of the detector tends to make a curve like (1a) look like (2a). We believe this effect is small. A more detailed examination of this point will be made in a later paper.

Accept equation (2a). Define the relaxation time,  $\underline{T}$ , as  $1/k_{10}(CO)$ . From the equation there is a point of inflection,  $d^2(CO^{**})/dt^2 = 0$  at  $(CO^{**}) = (CO)_{\infty}^{**}/4$ . On both sides of this point, the curve is almost linear and the slope is  $2/\underline{T}$ . Values of  $\underline{T}$  so obtained are presented in Table 2.

Table 2. Relaxation Time Measurements

Initial Pressure of CO atm	$\frac{v_1}{v_K}$	$\frac{v_r}{v_K}$	$\frac{\pi_t}{\pi_r}$	$\Delta_t$	$\frac{P_r}{\text{atm}}$	$\frac{\tau}{\mu\text{sec}}$	$\frac{\tau P_r}{\mu\text{sec atm}}$
.0560	10	1446	53.7	11.01	3.01	273	836
.0433	10	1446	53.7	11.01	2.62	246	645
.0713	7.7	1395	50.6	10.77	3.63	163	610
.0469	14	1453	54.2	11.04	2.54	237	601
.0311	11	1447	53.7	11.01	1.67	352	538
.0484	10	1433	52.0	10.95	2.56	224	573
.0313	15	1455	54.0	11.05	1.73	327	565
.0317	10	1445	53.6	11.00	1.70	325	552
.0403	12	1451	54.0	11.03	2.13	243	540
.0306	35	1500	57.0	11.23	1.74	234	407
.0243	30	1724	70.3	12.19	1.74	183	319
.0132	1112	2150	97.6	13.54	1.73	132	234
.0216	1012	1916	82.3	12.84	1.73	93	174
.0215	1015	1921	82.7	12.87	1.73	97	172
.0179	1122	2170	98.9	13.60	1.77	67	119
.0181	1100	2117	95.4	13.45	1.73	66	104
.0062	14.5	2935	153.0	15.33	0.95	37	35
.0060	14.5	2935	153.0	15.33	0.92	37	34

The mean value of the measurements in the vicinity of 1400°K, converted to 1400°K and 1 atm pressure, is

$$\underline{T} = 650 \pm 50 \text{ microseconds}$$

The form of pressure and temperature dependence used in making these conversions will be discussed below.  $\underline{T}$  may also be obtained from the slope of the straight line in Fig. 3 which has the advantage of using the whole curve. Within the limits of accuracy both methods gave the same results in several cases and the less laborious inflection point method was therefore adopted.

Pressure dependence of  $\underline{T}$ . For a collisional process, a simple inverse pressure dependence is to be expected. A graph of  $T_P$  versus  $p$  for those experiments close to 1400°K is shown in Fig. 4. The values of  $\underline{T}$  have been converted to 1400°K. A reasonable fit to a straight line is obtained.

Fig. 4 here

Temperature dependence of  $\underline{T}$ . The relaxation times are observed to decrease with increasing temperature as expected. The usual theories of vibrational relaxation lead to an expression of the form,

$$\log \underline{T} = \underline{A}T^{-1/3} + \underline{B} \quad (4)$$

where  $\underline{A}$  and  $\underline{B}$  are constants. Values of  $\log \underline{T}$  versus  $T^{-1/3}$  for the present observations are plotted in Fig. 5. The best straight line that

Fig. 5 here

can be drawn through the experimental points leads to  $\underline{A} = 64.45$  and  $\underline{B} = -2.943$

Equation (3) and the above value of  $\underline{A}$  were used in making the conversions of  $\underline{T}$  to 1400°K mentioned earlier.

The effect of impurities. The effect of small amounts of added  $H_2O$  or  $CO_2$  on the relaxation time of  $CO$  is shown in Table 3. Water causes

Table 3. Effect of Impurities on Vibrational Relaxation of CO

Composition of gas	Coolant in Trap	$T_r$ °K	$P_r$ atm	$\tau$ μsec	$\frac{\tau_p}{\mu sec atm}$
pure CO*	dry ice	1437	1.74	193	344
pure CO*	melting methylene bromide	1437	1.72	210	361
CO + .002% H <sub>2</sub> O	dry ice	1393	1.61	212	341
CO + .3% H <sub>2</sub> O	melting methylene bromide	1450	1.70	35	60
CO + .1% CO <sub>2</sub>	dry ice	1451	1.70	150	222
CO + .03% H <sub>2</sub> with < .04% CO <sub>2</sub>	liq N <sub>2</sub>	1404	1.24	173	270

\* Control runs with pure gas.

a marked increase in the rate of relaxation even in trace amounts. At a relative concentration of 3 parts in  $10^3$  the value of  $\tau$  is reduced by at least a factor of six. The reduction may be somewhat greater because the observed time is close to the response time of the detector. For  $\text{CO}_2$  a ratio of 1 part in  $10^3$  reduces  $\tau$  by about a factor of two-thirds. The experiment with the Matheson Reagent Grade CO gave relaxation times of about half those observed with the fractionally distilled samples. Since the  $\text{CO}_2$  impurity was removed by the  $-196^\circ\text{C}$  trap, this may be due to the hydrogen impurity.

#### Conclusions

1. The value reported here,  $\tau = 550 \mu\text{sec}$  at  $1470^\circ\text{K}$ , is 30 times greater than that given in our preliminary report.<sup>4</sup> The value at  $2200^\circ$  ( $150 \mu\text{sec}$ ) is greater than the value of  $10 \mu\text{sec}$  given in a preliminary report by the Princeton group.<sup>3</sup> This is presumably a matter of the removal of impurities. It is of course possible that even the present results are affected by impurities.

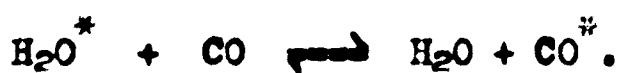
At present one may say that CO has the longest vibrational relaxation times known at any given temperature.

2. The experimental data favor hypotheses (2) and/or (3) over (1). Theory very strongly seconds the notion,<sup>1</sup> in that the interconversion of a large amount of energy between vibration and translation, as in reaction (1), is predicted to be extremely improbable ( $\sim 10^{-7}$  less probable than process (2) in the present instance).

We have made preliminary calculations of the rate constants  $k_{10}$  and  $\epsilon$  for equations (2) and (3) above according to the Schwartz, Slawsky, Herz-

field theory<sup>1</sup> as amended by Tanczoc.<sup>10</sup> For the Lennard-Jones parameter,  $\sigma$  for CO, we use 3.59 Å.<sup>11</sup> We calculate, at 1400°K,  $k_{10} = 1.9 \times 10^{-6} \text{ Z}$ ,  $k_{01} = 2.1 \times 10^{-7} \text{ Z}$ ,  $\epsilon = 4.3 \times 10^{-3} \text{ Z}$ . Z is the gas kinetic theory collision number. The experimental  $\gamma$  at 1400°K corresponds to  $k_{10} = 5 \times 10^{-7} \text{ Z}$ . The agreement between theory and experiment is as good as can be expected. Note that although  $\epsilon$  is calculated to be about  $10^3$  greater than  $k_{10}$ , the discussion given earlier indicates that the energy transfer at exact resonance probably does not affect the kinetics of the population of the various vibrational states significantly.

3. The vibrational relaxation time of CO is greatly diminished by the impurities H<sub>2</sub>O and CO<sub>2</sub>. These molecules have shorter vibrational relaxation times, and we suggest that the principal process is the highly efficient transfer of vibrational energy from one species to the other:



4. The infrared method for measuring vibrational relaxation times has the advantage of looking, at least to some extent, at the rate of excitation of particular states. The limitations as to rise time and sensitivity of detectors presently available are such that the method is applicable only to infra-red active molecules with rather long relaxation times.

#### Acknowledgments

We are indebted to the ONR for support. Dr. Russ Duff of Los Alamos generously performed many of the reflected shock calculations.

One of us (M.W.) is indebted to the Commissioners for the Exhibition of 1851 for a Senior Studentship, and one of us (R.T.) is indebted to the duPont Co. for a fellowship.

References

1. K. Herzfeld, Thermodynamics and Physics of Matter, Princeton University Press, 1955, Section H
2. V. Blackman, J. Fluid Mech. 1, 61 (1956)
3. P. V. Slobodskaya, Invest. Akad. Nauk. S.S.R., Ser. fiz. 12, 656 (1948)
4. M. W. Windsor, N. Davidson and R. Taylor, J. Chem. Phys. 27, 315 (1957)
5. S. Penner and D. Weber, J. Chem. Phys. 19, 807, 817 (1951)
6. S. Penner and D. Weber, J. Chem. Phys. 19, 1351, 1361 (1951)
7. D. Britton, N. Davidson and G. Schott, Discussions of the Faraday Society, No. 17, 1954, pp. 58-68
8. W. D. Greenspan and V. H. Blackman, Bull. Am. Phys. Soc. II, 217 (1957) (April 1957, Washington meeting)
9. E. Montroll and K. E. Shuler, J. Chem. Phys. 26, 454 (1957).
10. P. I. Tanezos, J. Chem. Phys. 25, 439 (1956)
11. J. O. Hirschfelder, C. F. Curtiss, and R. B. Bird, Molecular Theory of Gases and Liquids, J. Wiley and Sons, Inc., New York, 1954, p. 1111.

Legends for Figures

Fig. 1. Schematic Diagram of Equipment.

Fig. 2. Typical Oscillograph Record of Emission from CO heated by Shock.

Initial condition;  $T = 298^{\circ}\text{K}$ ;  $P = .056$  atm CO. Final condition,  $T = 1446^{\circ}\text{K}$ ,  $P = 3.01$  atm. Time is the horizontal coordinate. The three horizontal sweeps at the top, middle, and bottom of the picture are time calibration marks with 100  $\mu\text{sec}$  pipe. Emission of CO increases vertically.

Fig. 3. One-step versus Two-step Relaxation Processes.

Fig. 4. Pressure Dependence of Vibrational Relaxation in CO.

Fig. 5. Temperature Dependence of Vibrational Relaxation in CO.

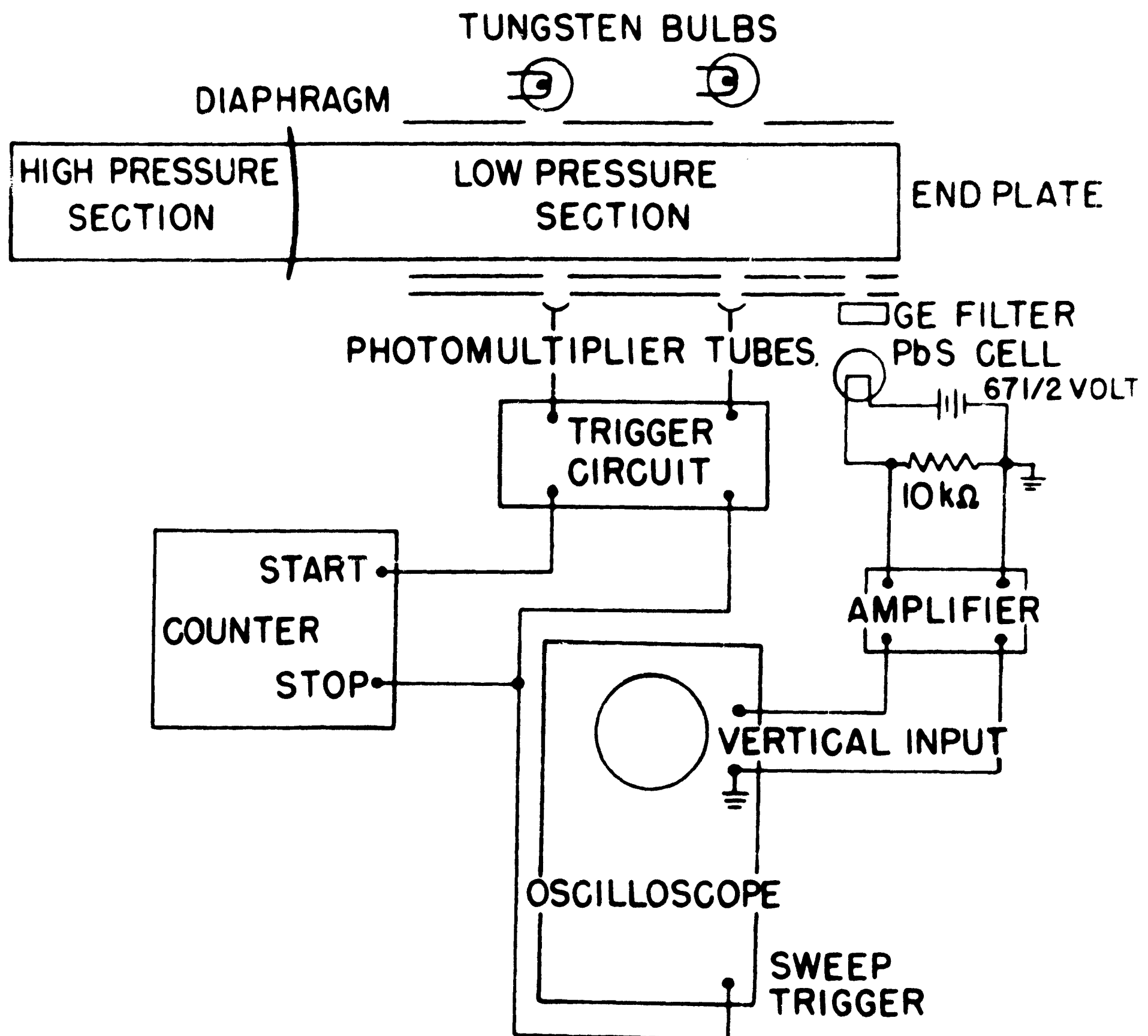


Fig 1



Fig. 2

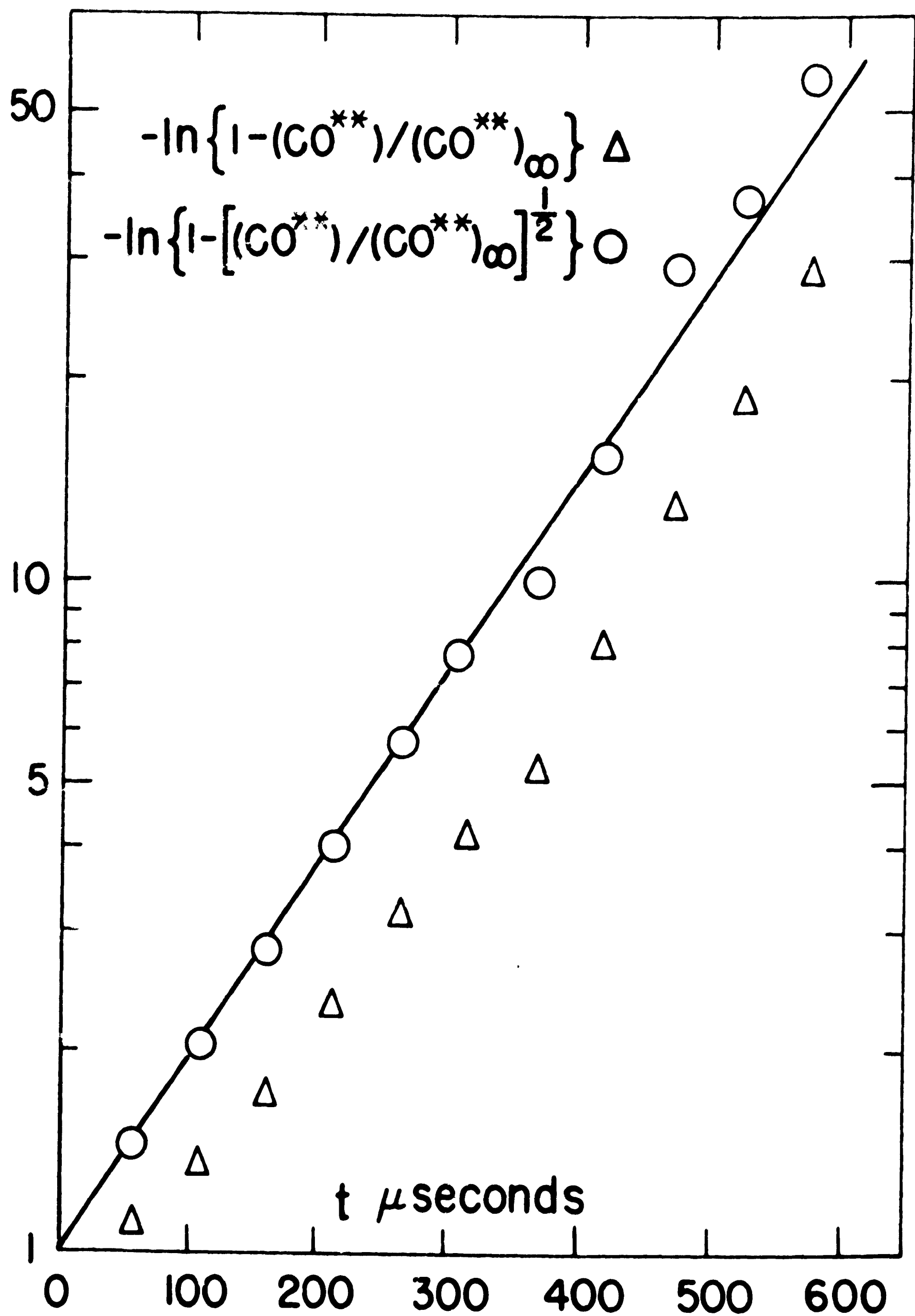


Fig.3

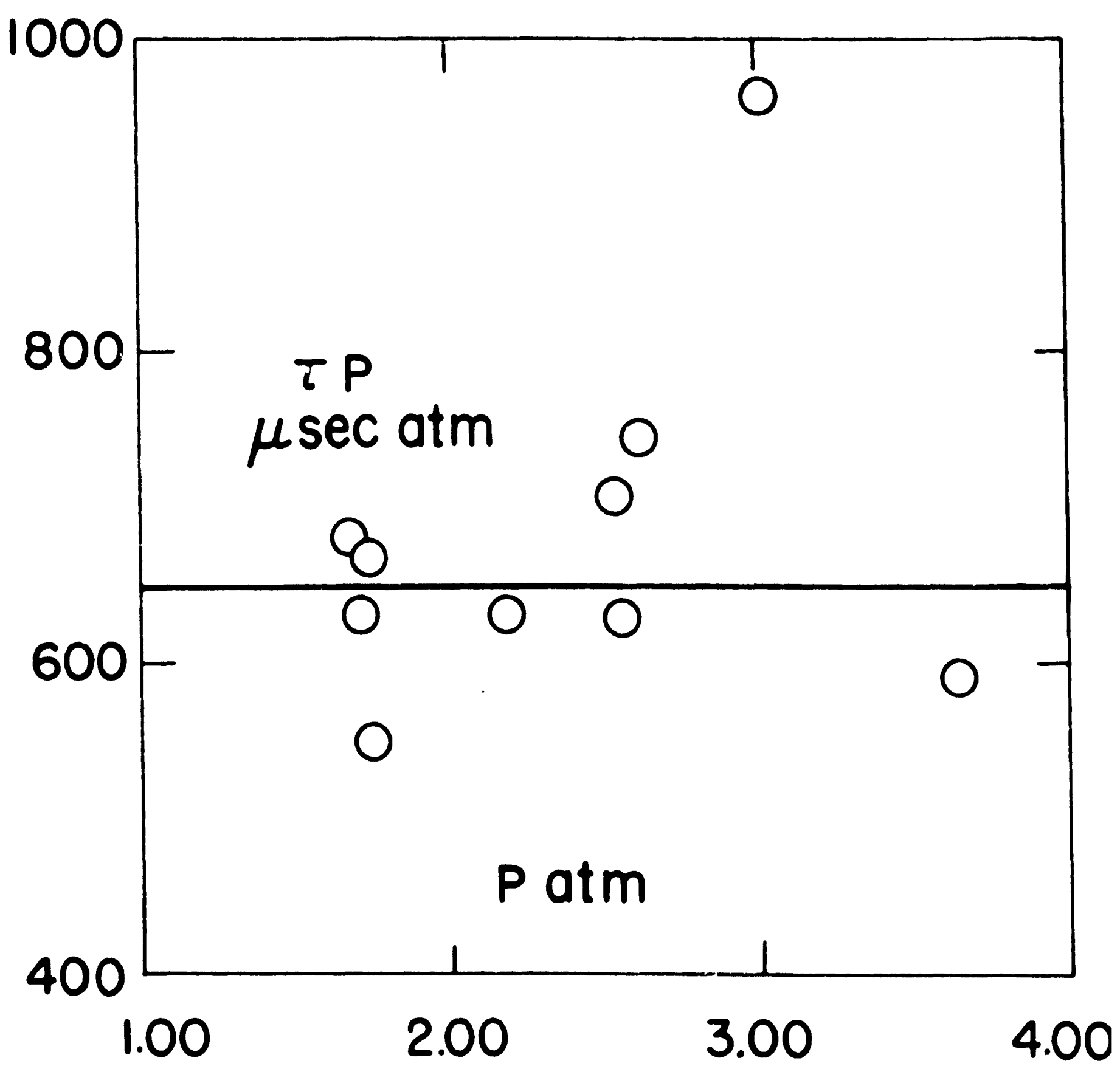


Fig. 4

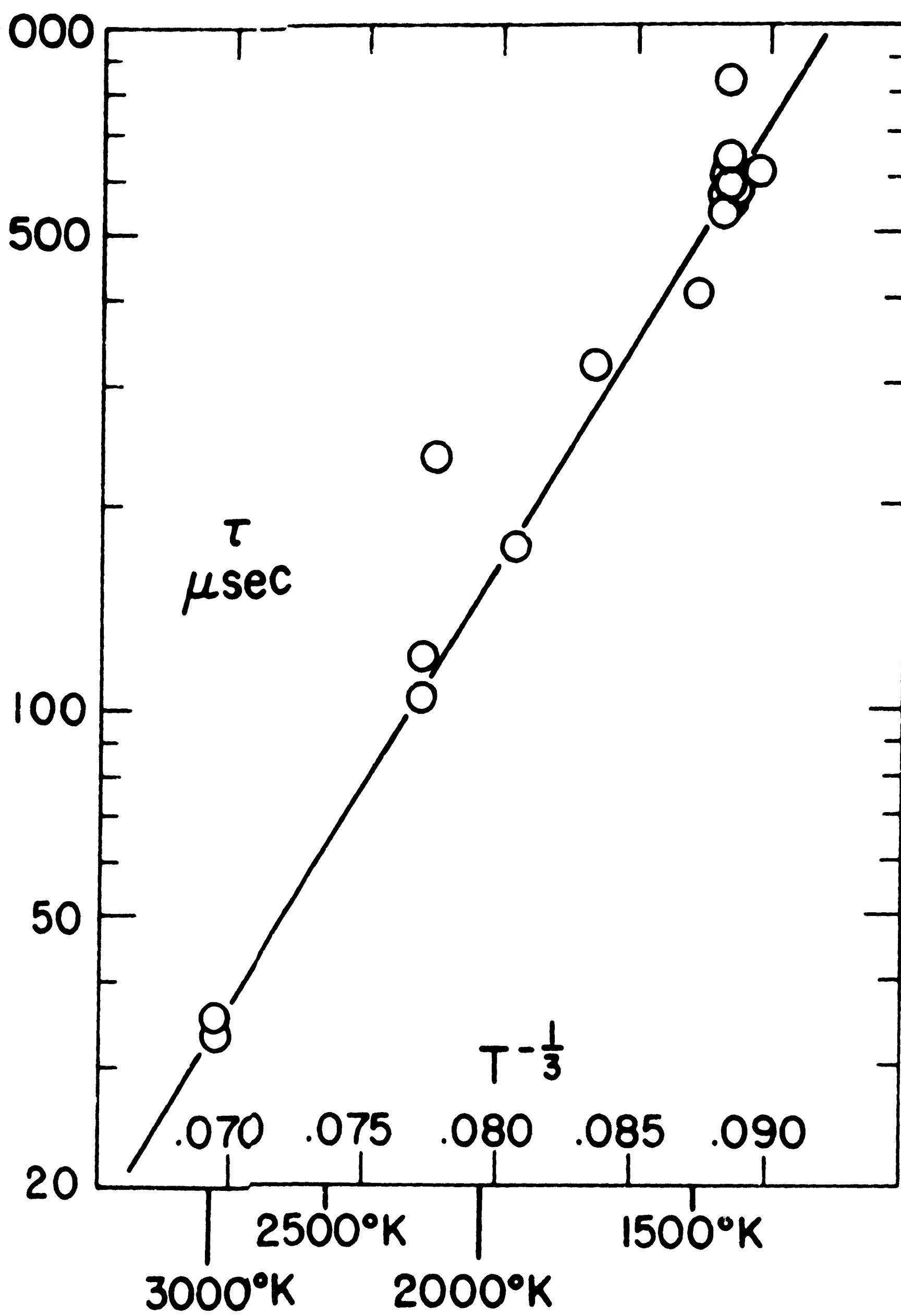


Fig. 5